Inorg. Chem. **2007**, *46*, 3049–3056

Antiferromagnetic or Canted Antiferromagnetic Orderings of Fe(III) d Spins of FeX_4^- Ions in BEDT-TTFVO(S)·FeX_4 (X = Cl, Br) [BEDT-TTFVO(S) = Bis(ethylenedithio)tetrathiafulvalenoquinone(-thioquinone)-1,3-dithiolemethide]

Mingxing Wang,[†,‡] Xunwen Xiao,[†,‡] Hideki Fujiwara,*[,†,‡] Toyonari Sugimoto,*[,†,‡] Satoru Noguchi,*[,‡,§] Takekazu Ishida,[‡,§] Takehiko Mori,*[,∥] and Hiroko Aruga Katori[⊥]

Department of Chemistry, Graduate School of Science, Osaka Prefecture University, Osaka 599-8570, Japan, CREST, Japan Science and Technology Agency, Saitama 332-0012, Japan, Department of Physics and Electronics, Graduate School of Engineering, Osaka Prefecture University, Osaka 599-8531, Japan, Department of Organic and Polymeric Materials, Graduate School of Science and Technology, Tokyo Institute of Technology, Tokyo 152-8552, Japan, and RIKEN (The Institute of Physical and Chemical Research), Saitama 351-0198, Japan

Received September 19, 2006

By the reaction of new donor molecules, bis(ethylenedithio)tetrathiafulvalenoquinone(-thioquinone)-1,3-dithiolemethides [BEDT-TTFVO (**1**) and BEDT-TTFVS (**2**)] with FeX_3 (X = Cl, Br) in CS_2/CH_3CN, 1:1 salts of **1** or **2** with an FeX_4^- ion (**1**·FeX_4 and **2**·FeX_4) were obtained as black needle crystals. Their crystal structures are very similar to each other, in which the donor molecules are strongly dimerized and the dimers construct a one-dimensional uniform chain along the *a* axis, while the FeX_4^- ions are located at an open space surrounded by the neighboring donor molecules and also construct a one-dimensional uniform chain along the *a* axis. There are close contacts between the donor molecules and the FeX_4^- ions and significant differences in the contact distances among the four salts. All of the salts are semiconductors with room-temperature electrical conductivities of 10^{-4}–10^{-2} S cm^{-1}. The Fe(III) d spins of the FeX_4^- ions are subject to dominant ferromagnetic interaction through the participation of one of the singlet π spins to form a short-range ferromagnetic d-spin chain. Such neighboring chains interact antiferromagnetically with each other through the singlet π spins and are ordered at 1.0, 2.4, and 0.8 K for **1**·$FeCl_4$, **1**·$FeBr_4$, and **2**·$FeCl_4$, respectively. On the other hand, the antiferromagnetic ordering occurred with some canted angle at 1.9 K to leave a small magnetization for **2**·$FeBr_4$.

1. Introduction

Much attention still continues to be directed toward developing magnetic molecular conductors with significant interactions between conducting electrons and localized spins both involved in the systems,[1] because the simultaneous appearance of a metallic conductivity and a ferromagnetic ordering based on the significant interactions between the two components, that is, a genuine ferromagnetic molecular metal, has not been achieved yet.[2] An approach to the final objective has been attempted chiefly using a variety of cation radical (CR) salts composed of π-donor molecules and magnetic counteranions with π, d, or f spins, both of which *usually* form such layers as to be stacked alternately in the crystals. Accordingly, the interactions between the two

* To whom correspondence should be addressed. E-mail: hfuji@c.s.osakafu-u.ac.jp (H.F.), toyonari@c.s.osakafu-u.ac.jp (T.S.), noguchi@pe.osakafu-u.ac.jp (S.N.), takehiko@o.cc.titech.ac.jp (T.M.).

† Department of Chemistry, Graduate School of Science, Osaka Prefecture University.

‡ CREST, Japan Science and Technology Agency.

§ Department of Physics and Electronics, Graduate School of Engineering, Osaka Prefecture University.

∥ Tokyo Institute of Technology.

⊥ RIKEN.

(1) (a) Day, P.; Kurmoo, M.; Mallah, T.; Marsden, I. R.; Friend, R. H.; Pratt, F. L.; Hayes, W.; Chasseau, D.; Gaultier, J.; Bravic, G.; Ducasse, L. *J. Am. Chem. Soc.* **1992**, *114*, 10722−10729. (b) Coronado, E.; Day, P. *Chem. Rev.* **2004**, *104*, 5419−5448. (c) Ouahab, L.; Enoki, T. *Eur. Inorg. Chem.* **2004**, 933−941. (d) Kurmoo, M.; Graham, A. W.; Day, P.; Coles, S. J.; Hursthouse, M. B.; Caulfield, J. L.; Singleton, J.; Pratt, F. L.; Hayes, W.; Ducasse, L.; Guinonneau, P. *J. Am. Chem. Soc.* **1995**, *117*, 12209−12217.

(2) Coronado, E.; Galán Mascarós, J. R.; Gómez Garciá, C. J.; Laukhin, V. N. *Nature* **2000**, *408*, 447−449.

10.1021/ic0617700 CCC: $37.00
Published on Web 03/23/2007

components can occur only at the interface between two neighboring layers of the donor molecules and magnetic counteranions. In a lot of the CR salts with such an alternate layer structure obtained so far, metal-to-insulator transitions preferentially occurred, and novel physical phenomena that originate from the $\pi-$d interactions were observed only in the temperature range of the insulating states.[3] Nevertheless, in some CR salts, metallic conductivities were maintained down to low temperatures, but the observed $\pi-$d interactions were not so large.[4] Only one exceptional example that demonstrates the strong $\pi-$d interaction was obtained in a λ-(BETS)$_2$·$FeCl_4$ salt [BETS = bis(ethylenedithio)tetraselenafulvalene] with an $FeCl_4^-$ ion that possesses Fe(III) d spins. In this salt, a metallic conductivity was maintained above 8 K, but at 8 K, it changed suddenly to the insulating state as a result of the strong $\pi-$d interaction between one Se atom in the BETS molecule and one Cl atom in the $FeCl_4^-$ ion.[5]

All of the π-donor molecules that are derived from tetrathiafulvalene (TTF), tetraselenafulvalene, and tetrathiafulvalenoquinone(-thioquinone)-1,3-dithiolemethides synthesized by our group and are used in the formation of CR salts[6] have their highest occupied molecular orbitals (HOMOs) with the largest electron densities at the central tetrathiaethylene and tetraselenaethylene moieties. Accordingly, in order to achieve stronger $\pi-$d interactions, it is necessary to construct the close contacts between S or Se atoms in the central tetrathiaethylene or tetraselenaethylene moieties and the counteranion ligands. To prepare CR salts with such a stacking structure that counteranions are preferentially located near the central part of donor molecules, we noticed ethylenedithiotetrathiafulvalenoquinone(-thioquinone)-1,3-dithiolemethides substituted with an additional ethylenedithio group [BEDT-TTFVO (**1**) and BEDT-TTFVS (**2**)]. These

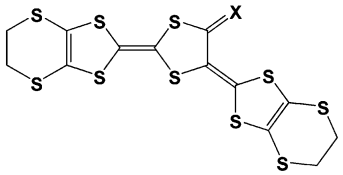

1 X = O : BEDT-TTFVO
2 X = S : BEDT-TTFVS

new donor molecules could be readily synthesized, and their CR salts with $FeCl_4^-$ and $FeBr_4^-$ ions were also obtained. As expected, the counteranions were located near the central part of molecule **1** or **2** in their crystals, but unfortunately the composition of the donor molecule and the counteranion was 1:1, so that all of the CR salts exhibited low electrical conductivities. Nevertheless, their magnetic properties gave very interesting results. Thus, short-range ferromagnetic d-spin chains were formed in all of the CR salts, and with decreasing temperature, such a pair of ferromagnetic chains were antiferromagnetically coupled through the dimer of the donor molecules with each other to bring about antiferromagnetic ordering in **1**·$FeCl_4$, **2**·$FeCl_4$, and **1**·$FeBr_4$. Very interestingly, for **2**·$FeBr_4$,[7] a small magnetization was observed because antiferromagnetic ordering occurred with some canted angle.[8] To our knowledge, this canted antiferromagnetism due to short-range ferromagnetic d-spin chains provides the first case in molecular systems, in which short-range spin chains are antiferromagnetic so far. This paper reports the crystal structures, electrical conductivities, and magnetic properties of **1**·$FeCl_4$, **2**·$FeCl_4$, **1**·$FeBr_4$, and **2**·$FeBr_4$ and discusses the plausible formation mechanism of this short-range ferromagnetic d-spin chain in all of the CR salts and the appearance of a canted antiferromagnetic ordering and also another magnetic ordering for **2**·$FeBr_4$.

2. Experimental Section

Synthesis of 1, 2, 1·FeX_4, and 2·FeX_4 (X = Cl, Br). Donor **2** was synthesized according to our previous procedure.[9] Thus, 4,5-ethylenedithio-4′,5′-bis(cyanoethylthio)tetrathiafulvalene (330 mg, 0.71 mmol) was converted to a bis(tetra-*n*-butylammonium, *n*-Bu_4N^+) salt of a dianionic bis(4,5-ethylenedithiotetrathiafulvalene-4′,5′-dithiolato)zinc complex by successive treatment with sodium (360 mg, 15.6 mmol), $ZnCl_2$ (96 mg, 0.71 mmol), and *n*-Bu_4NBr (455 mg, 1.42 mmol) in MeOH (20 mL). This salt was again reacted with 2-methyl-4,5-ethylenedithio-1,3-dithiolanium tetrafluoroborate (463 mg, 1.42 mmol) in tetrahydrofuran (THF)/*N*,*N*-dimethylformamide (DMF) (30 mL, 1:1, v/v) at −78 °C under argon and warmed to room temperature overnight. After separation of the reaction mixture by column chromatography on silica gel, followed by recrystallization from CS_2/*n*-hexane, **2** (146 mg, 0.28 mmol) was obtained as a black powder [mp 233−235 °C (dec)] in an overall yield of 40%. The reaction of **2** with mercury(II) acetate (890 mg, 2.8 mmol) in THF/AcOH (3:1, v/v) at room temperature under argon gave **1** (130 mg, 0.26 mmol) as a red powder (mp 237−239 °C) in 91% after recrystallization from CS_2/*n*-hexane. The MS and ^{1}H NMR ($CDCl_3$) spectral results were as follows: *m*/*z* 500 (M^+) and δ 3.30 (s, 4H), 3.37 (s, 4H) for **1** and *m*/*z* 516 (M^+) and δ 3.29 (s, 4H), 3.40 (s, 4H) for **2**. The FeX_4^- (X = Cl, Br) salts of **1** and

(3) (a) Enomoto, K.; Miyazaki, A.; Enoki, T. *Synth. Met.* **2001**, *120*, 977−978. (b) Matsumoto, T.; Kominami, T.; Ueda, K.; Sugimoto, T.; Tada, T.; Noguchi, S.; Yoshino, H.; Murata, K.; Shiro, M.; Negishi, E.; Toyota, N.; Endo, S.; Takahashi, K. *Inorg. Chem.* **2002**, *41*, 4763−4769. (c) Enoki, T.; Yamazaki, H.; Nishijo, J.; Miyazaki, A.; Ugawa, K.; Ogura, E.; Kuwatani, Y.; Iyoda, M.; Sushko, Y. V. *Synth. Met.* **2003**, *137*, 1173−1174. (d) Matsumoto, T.; Sugimoto, T.; Aruga Katori, H.; Noguchi, S.; Ishida, T. *Inorg. Chem.* **2004**, *43*, 3780−3782. (e) Hiraoka, T.; Kamada, Y.; Matsumoto, T.; Fujiwara, H.; Sugimoto, T.; Noguchi, S.; Ishida, T.; Nakazumi, H.; Aruga Katori, H. *J. Mater. Chem.* **2005**, *15*, 3479−3487. (f) Nishijo, J.; Miyazaki, A.; Enoki, T.; Watanabe, R.; Kuwatani, Y.; Iyoda, M. *Inorg. Chem.* **2005**, *44*, 2493−2506.

(4) (a) Ojima, E.; Fujiwara, H.; Kato, K.; Kobayashi, H.; Tanaka, H.; Kobayashi, A.; Tokumoto, M.; Cassoux, P. *J. Am Chem. Soc.* **1999**, *121*, 5581−5582. (b) Otsuka, T.; Kobayashi, A.; Miyamoto, Y.; Kikuchi, J.; Wada, N.; Ojima, E.; Fujiwara, H.; Kobayashi, H. *Chem. Lett.* **2000**, 732−733. (c) Fujiwara, H.; Wada, K.; Hiraoka, T.; Hayashi, T.; Sugimoto, T.; Nakazumi, H.; Yokogawa, K.; Teramura, M.; Yasuzuka, S.; Murata, K.; Mori, T. *J. Am. Chem. Soc.* **2005**, *127*, 14166−14167. (d) Fujiwara, H.; Hayashi, T.; Sugimoto, T.; Nakazumi, H.; Noguchi, S.; Li, L.; Yokogawa, K.; Yasuzuka, S.; Murata, K.; Mori, T. *Inorg. Chem.* **2006**, *45*, 5712−5714.

(5) Kobayashi, H.; Tomita, T.; Naito, A.; Kobayashi, A.; Sakai, F.; Watanabe, T.; Cassoux, P. *J. Am. Chem. Soc.* **1996**, *118*, 368−377.

(6) Yamada, J.; Sugimoto, T. *TTF Chemistry—Fundamentals and Applications of Tetrathiafulvalene*; Kodansha & Springer: Tokyo, Berlin, Heidelberg, New York, 2004.

(7) Wang, M. X.; Fujiwara, H.; Sugimoto, T.; Noguchi, S.; Ishida, T. *Inorg. Chem.* **2005**, *44*, 1184−1186.

(8) Moriya, T. *Magnetism I*; Academic Press: New York, 1963.

(9) Iwamatsu, M.; Kominami, T.; Ueda, K.; Sugimoto, T.; Fujita, H.; Adachi, T. *Chem. Lett.* **1999**, 329−330.

2 were obtained by the reaction of **1** or **2** with FeX_3 using the three-phase contact method developed by our group.[10] Thus, to a solution of **1** or **2** (1 mg) in CS_2 (5 mL) was gently added CH_3CN (2 mL) and, furthermore, a solution of FeX_3 (40 mg) in CH_3CN (5 mL). When the three-phase solution was kept at room temperature for ca. 2 weeks, black needle crystals of **1**·FeX_4 (mp >300 °C) and **2**·FeX_4 (mp >300 °C) appeared at the interface between the upper two phases. The ratio of molecule **1** or **2** and FeX_4^- ion in the salts was determined to be 1:1 from their X-ray structure analyses. The $GaBr_4^-$ salt of **2**, **2**·$GaBr_4$ (mp >300 °C), was also obtained by the above method.

X-ray Data Collection, Structure Solution, and Refinement. The X-ray diffraction data were collected for a single crystal of **2**·$FeBr_4$ on a Rigaku RAXIS-RAPID imaging plate diffractometer with a graphite-monochromated Mo Kα radiation ($\lambda = 0.7107$ Å) and for single crystals of $\mathbf{1}_2$·$FeCl_4$, $\mathbf{1}_2$·$FeBr_4$, and **2**·$FeCl_4$ on a Rigaku AFC-8 Mercury CCD diffractometer with a confocal X-ray mirror system (Mo Kα radiation; $\lambda = 0.7107$ Å). The structures were solved by a direct method (*SIR92*),[11] expanded by *DIRDIF94*,[12] and refined on F^2 with full-matrix least-squares analysis. Calculated positions of the H atoms [d(C−H) = 0.95 Å] were included but not refined in the final calculations. All of the calculations were performed using the *CrystalStructure* crystallographic software package of the Molecular Structure Corp.[13]

Crystal data for 1·$FeCl_4$: $C_{13}H_8S_{10}OFeCl_4$, $M = 698.46$, monoclinic, $a = 6.298(2)$ Å, $b = 21.508(8)$ Å, $c = 17.948(7)$ Å, $\beta = 99.075(2)°$, $V = 2401(2)$ Å^3, $T = 293$ K, space group $P2_1/c$, $Z = 4$, μ(Mo Kα) = 19.49 cm^{-1}, 26 720 reflections measured, 26 302 unique ($R_{init} = 0.050$), of which 14 162 were used in all calculations [$F^2 > 2.00\sigma(F^2)$]. The final R and R_w were 0.038 and 0.038, respectively.

Crystal data for 2·$FeCl_4$: $C_{13}H_8S_{11}FeCl_4$, $M = 714.53$, monoclinic, $a = 6.367(6)$ Å, $b = 21.33(3)$ Å, $c = 18.45(2)$ Å, $\beta = 99.732(6)°$, $V = 2470(4)$ Å^3, $T = 293$ K, space group $P2_1/c$, $Z = 4$, μ(Mo Kα) = 19.22 cm^{-1}, 51 780 reflections measured, 6586 unique ($R_{init} = 0.077$), of which 3115 were used in all calculations [$F^2 > 2.00\sigma(F^2)$]. The final R and R_w were 0.051 and 0.051, respectively.

Crystal data for 1·$FeBr_4$: $C_{13}H_8S_{10}OFeBr_4$, $M = 876.27$, monoclinic, $a = 6.371(4)$ Å, $b = 21.565(13)$ Å, $c = 18.391(12)$ Å, $\beta = 98.807(3)°$, $V = 2497(3)$ Å^3, $T = 293$ K, space group $P2_1/c$, $Z = 4$, μ(Mo Kα) = 78.67 cm^{-1}, 55 340 reflections measured, 5916 unique ($R_{init} = 0.047$), of which 3061 were used in all calculations [$F^2 > 2.00\sigma(F^2)$]. The final R and R_w were 0.031 and 0.021, respectively.

Crystal data for 2·$FeBr_4$: $C_{13}H_8S_{11}FeBr_4$, $M = 892.33$, monoclinic, $a = 6.483(8)$ Å, $b = 21.523(4)$ Å, $c = 18.769(4)$ Å, $\beta = 99.394(3)°$, $V = 2583(3)$ Å^3, $T = 296$ K, space group $P2_1/c$, $Z = 4$, μ(Mo Kα) = 76.81 cm^{-1}, 11 428 reflections measured, 5714 unique, of which 2941 were used in all calculations [$F^2 > 2.00\sigma(F^2)$]. The final R and R_w were 0.035 and 0.048, respectively.

Electrical Conductivity, Magnetic, Electron Spin Resonance (ESR), and Heat Capacity Measurements. Electrical conductivities were measured on the single crystals of **1**·FeX_4 and **2**·FeX_4 in the temperature region of 77−298 K. Four gold electrodes (15 $\mu\varnothing$) were contacted with a gold paste in parallel with the largest plane of the needle crystals. The magnetizations were measured in the temperature range of 1.9−300 K under an applied field of 1 kOe with a SQUID magnetometer (MPMS XL; Quantum Design). The paramagnetic susceptibility (χ_p) was obtained by subtracting the diamagnetic contribution estimated using Pascal's constants[14] from the observed magnetic susceptibility. The magnetizations down to 0.4 K and also up to 300 kOe at 1.9 K were measured using a homemade pulsed-magnet system combined with a ^{3}He refrigerator by a conventional induction method. ESR measurement of **2**·$GaBr_4$ was performed in the temperature range of 20−300 K by use of a Bruker E500 spectrometer. The heat capacity of **2**·$FeBr_4$ was measured by a thermal relaxation method down to 0.5 K using a ^{3}He cryostat of a MagLab^{HC} microcalorimeter (Oxford Instruments).

3. Results and Discussion

3.1. Crystal Structures of 1·$FeCl_4$, 2·$FeCl_4$, 1·$FeBr_4$, and 2·$FeBr_4$. The four crystals of **1**·$FeCl_4$, **2**·$FeCl_4$, **1**·$FeBr_4$, and **2**·$FeBr_4$ are isostructural to each other, although there are slight differences in the contact distances between the donor molecules, between the counteranions, and between the donor molecule and the counteranion. As a representative, the crystal structure of **1**·$FeCl_4$ is shown in Figure 1. The donor molecule in each crystal has a high planarity in spite of a slightly large torsional angle of 8.6−10.7° between the terminal 1,3-dithiole ring and the TTF skeleton. The donor molecules form a strongly dimerized structure with several shorter S···S contacts (3.40 and 3.57 Å for **1**·$FeCl_4$, 3.47 and 3.60 Å for **2**·$FeCl_4$, 3.37 and 3.54 Å for **1**·$FeBr_4$, and 3.41 and 3.55 Å for **2**·$FeBr_4$) than the sum of the van der Waals (vdw) radii of two S atoms (3.70 Å).[15] Each dimer is stacked with each other in a one-dimensional manner along the a axis with several S···S contacts. Such donor stacks are not arranged in line but in a zigzag manner along the c axis, so that the $FeCl_4^-$ or $FeBr_4^-$ ions are located at open spaces surrounded by the neighboring donor molecules and construct a one-dimensional and uniform chain along the a axis with slightly longer Cl···Cl (3.91−4.12 Å for **1**·$FeCl_4$ and 3.96−4.23 Å for **2**·$FeCl_4$) or Br···Br (3.99−4.06 Å for **1**·$FeBr_4$ and 4.04−4.18 Å for **2**·$FeBr_4$) distances than the sum of the vdw radii of two Cl or Br atoms (3.60 or 3.90 Å).[15] In addition, there are several Cl···S (3.42 Å for **1**·$FeCl_4$ and 3.45 Å for **2**·$FeCl_4$) or Br···S (3.52−3.76 Å for **1**·$FeBr_4$ and 3.58−3.78 Å for **2**·$FeBr_4$) contacts with shorter distances than the sum of the vdw radii of Cl and S atoms (3.65 Å)[15] and of Br and S atoms (3.80 Å)[15] between the donor molecule and the counteranion. The close Cl···Cl and Cl···S and also Br·Br and Br···S contacts suggest significant d−d and π−d interactions in these salts. These intermolecular S···S, X···X, and X···S (X = Cl, Br) contacts in **1**·$FeCl_4$ and **1**·$FeBr_4$ are shorter than those in **2**·$FeCl_4$ and **2**·$FeBr_4$ as a whole and suggest that both d−d and π−d interactions in the salts based

(10) Kominami, T.; Matsumoto, T.; Ueda, K.; Sugimoto, T.; Murata, K.; Shiro, M.; Fujita, H. *J. Mater. Chem.* **2001**, *11*, 2089−2094.
(11) Altomare, A.; Burlea, M. C.; Gamalli, M.; Cascarano, G. L.; Giacovazzo, C.; Guagliardi, A.; Polidre, G. *J. Appl. Crystallogr.* **1994**, *27*, 435.
(12) Beurskens, P. T.; Admiraal, G.; Beurskens, G.; Bosman, W. P.; de Gelder, D.; Israel, R.; Smith, J. M. M. *Technical Report of the Crystallography Laboratory*; University of Nijmegen: Nijmegen, The Netherlands, 1994.
(13) *CrystalStructure Analysis Package*; Molecular Structure Corp.: Houston, TX, 1992.
(14) König, E. *Landolt Bornstein, Group II: Atomic and Molecular Physics, Vol. 2, Magnetic Properties of Coordination and Organometallic Transition Metal Compounds*; Spring Verlag: Berlin, 1966.
(15) Pauling L. *The Nature of the Chemical Bond*, 3rd ed.; Cornell University Press: Ithaca, NY, 1960.

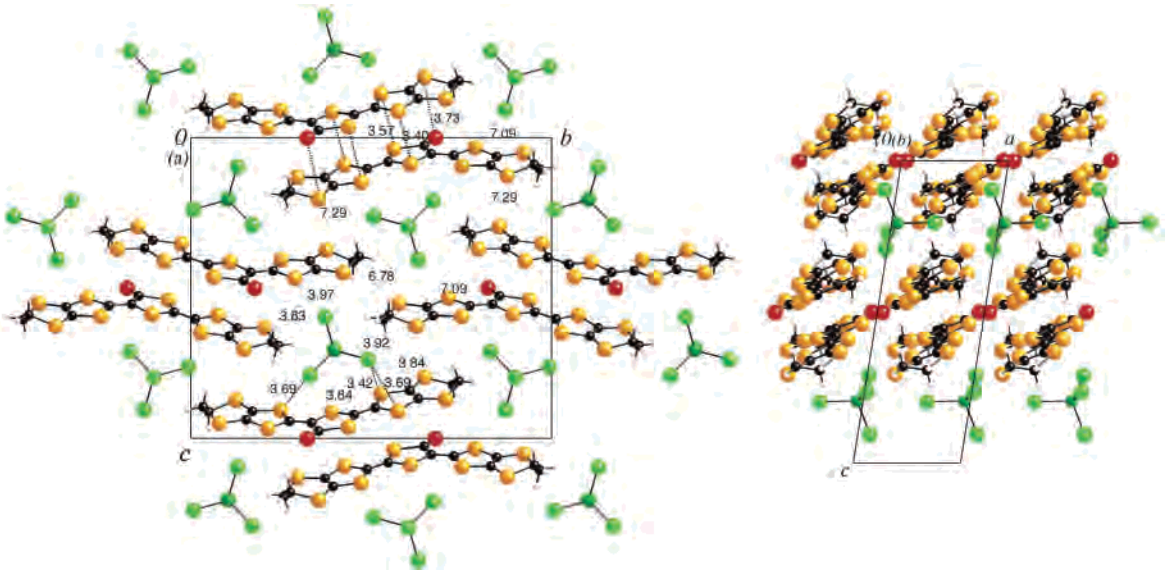

Figure 1. Projections of the crystal structure of **1**·$FeCl_4$ to the *bc* and *ac* planes.

on **1** are stronger than those in the salts based on **2** because of smaller vdw radii of the S atom than that of the O atom.

3.2. Electrical Conductivities. The electrical conductivities measured on the single crystals of **1**·$FeCl_4$, **2**·$FeCl_4$, **1**·$FeBr_4$, and **2**·$FeBr_4$ were 3×10^{-4}, 3×10^{-4}, 3×10^{-2}, and 4×10^{-2} S cm^{-1} at room temperature, respectively. All of the salts exhibited semiconducting behaviors in the temperature region measured. To presume a probable conduction pathway in these salts, the degree of π contacts between the donor molecules was investigated using extended Hückel MO calculations.[16] In each salt, five kinds of $\pi-\pi$ interactions (***c***, ***a***, ***p***, ***b1***, and ***b2***) are present (Figure 2) and their overlap integrals (*S*) were calculated using their crystal structure data, as shown in Table 1. The contact ***c*** has such a large *S* that a strong dimerization between neighboring donor molecules is formed. There are two different contacts, ***a*** and ***p***, between the donor dimers along *a* axis, and the former one is 2−4 times larger than the latter one. Because the contacts ***b1*** and ***b2*** are very small, it is most probable that each one-dimensional chain of the donor dimers along the *a* axis serves as the conduction pathway. To see this in more detail, the *S* values of the contacts ***a*** and ***p*** are on the whole larger for the $FeCl_4^-$ salts than for the $FeBr_4^-$ salts, expecting higher room-temperature conductivities for the $FeCl_4^-$ salts than for the $FeBr_4^-$ salts. However, the $FeBr_4^-$ salts practically showed higher conductivities by ca. 10^2 times than the $FeCl_4^-$ salts. This discrepancy may come from the different quality and/or conductivity measurements on the different crystal planes between both of the salts.

3.3. Ferromagnetic Interaction between the Fe(III) d Spins of the FeX_4^- Ions. The temperature dependences of magnetic susceptibilities (χ_p) for all of the salts obeyed a Curie−Weiss law [$\chi_p = C/(T - \theta)$, where *C* is a Curie constant and θ is a Weiss temperature] in the temperature region of 10−20 to 300 K. The *C* values are 4.35−4.54 emu K mol^{-1} and are close to the value calculated as an entity of the Fe(III) ($S = {}^5/_2$) d spins of one $FeCl_4^-$ or $FeBr_4^-$ ion. The π spins on the radical cations of **1** or **2** are in the singlet state, and a singlet−triplet energy gap is estimated to be a large value of ca. 250 K from the temperature dependence of signal intensities by the ESR measurement of the corresponding **2**·$GaBr_4$ salt. Accordingly, there is no contribution to χ_p at all in the low-temperature region. The θ values are +1.8, +1.6, +3.7, and +3.4 K for **1**·$FeCl_4$, **2**·$FeCl_4$, **1**·$FeBr_4$, and **2**·$FeBr_4$, respectively, indicating a preferential ferromagnetic interaction between the Fe(III) d spins of the $FeCl_4^-$ or $FeBr_4^-$ ions for all of the salts. The donor π spins in the singlet state should also participate in the interaction between neighboring Fe(III) d spins. As shown in Figure 3, the χ_p values showed different temperature dependences for each salt. Thus, for **1**·$FeCl_4$ and **2**·$FeCl_4$, χ_p gradually became smaller than the values expected by the Curie−Weiss curves with $\theta = +1.7$ and +1.6 K in the lower temperature region than 10−20 K but continued to increase down to 1.9 K with decreasing temperature. Also for **1**·$FeBr_4$ and **2**·$FeBr_4$, a similar tendency was observed, but for **1**·$FeBr_4$, χ_p reached a maximum at 2.4 K, and below the temperature, it decreased sharply with decreasing temperature. This behavior indicates the occurrence of an antiferromagnetic ordering of the Fe(III) d spins of the $FeBr_4^-$ ions at 2.4 K. In contrast, for **2**·$FeBr_4$, χ_p still continued to increase with decreasing temperature and near 2 K, the lowest limit of temperature in this experiment, became constant. It is supposed that some kind of magnetic ordering occurs near this temperature, but it cannot be confirmed until the

Table 1. Overlap Integrals ($S \times 10^{-3}$) of $\pi-\pi$ Interactions (***c***, ***a***, ***p***, ***b1***, and ***b2***) between Neighboring Molecules **1** and **2** for **1**·$FeCl_4$, **2**·$FeCl_4$, **1**·$FeBr_4$, and **2**·$FeBr_4$

interaction	**1**·$FeCl_4$	**2**·$FeCl_4$	**1**·$FeBr_4$	**2**·$FeBr_4$
c	30.92	30.24	33.02	30.19
a	−12.31	−12.75	−11.19	−9.05
p	−3.23	−5.12	−3.77	−3.79
b1	−0.92	−0.70	−0.70	−0.76
b2	−0.05	−0.06	−0.05	−0.05

(16) Mori, T.; Kobayashi, A.; Sasaki, Y.; Kobayashi, H.; Saito, G.; Inokuchi, H. *Bull. Chem. Soc. Jpn.* **1984**, *57*, 627−633.

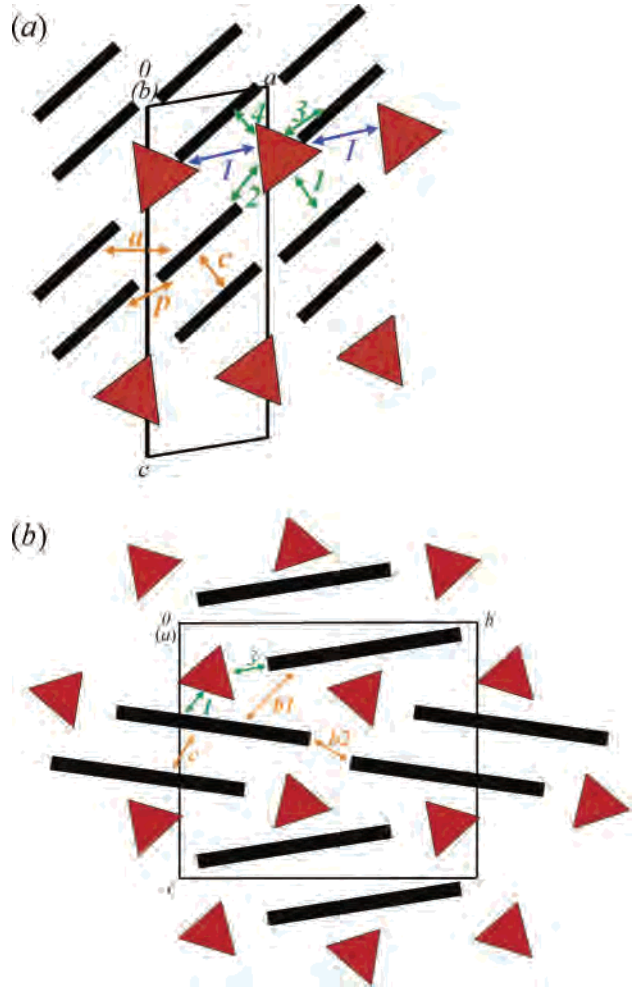

Figure 2. $\pi-\pi$ interactions (orange arrows: ***c***, ***a***, ***p***, ***b1***, and ***b2***) between neighboring molecules **1** and **2**, $\pi-$d interactions (green arrows: ***1***, ***2***, ***3***, and ***4***) between molecule **1** or **2** and the $FeCl_4^-$ or $FeBr_4^-$ ion, and d−d interaction (blue arrows: ***I***) between the $FeCl_4^-$ or $FeBr_4^-$ ions in the (a) *ac* and (b) *bc* planes. In these schematic drawings of the crystal structures, black rectangles and red triangles express donor molecule **1** or **2** and the $FeCl_4^-$ or $FeBr_4^-$ ion, respectively.

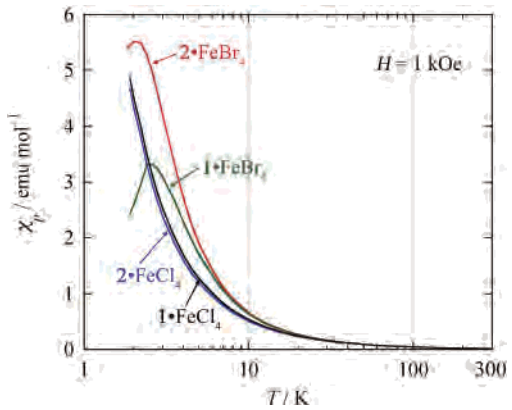

Figure 3. Temperature (T) dependences of magnetic susceptibilities (χ_p) measured at $H = 1$ kOe for **1**·$FeCl_4$ (black), **2**·$FeCl_4$ (blue), **1**·$FeBr_4$ (green), and **2**·$FeBr_4$ (red) in the T region of 1.9−300 K.

magnetic measurement down to much lower temperature is carried out.

The magnetic field (H) dependence of magnetization (M) (the $M-H$ curve) was measured in the H range up to 50 kOe at 1.9 K for each salt. In all of the cases, M tends to

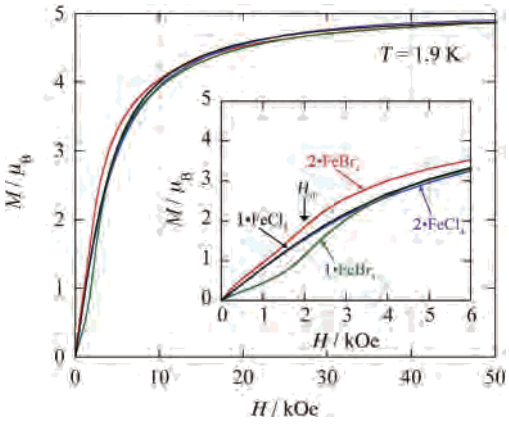

Figure 4. Field (H) dependences of magnetizations (M) measured at 1.9 K for **1**·$FeCl_4$ (black), **2**·$FeCl_4$ (blue), **1**·$FeBr_4$ (green), and **2**·$FeBr_4$ (red) in the H region up to 50 kOe. The inset shows an expansion in the lower H region below 6 kOe. A black arrow shows a spin-flop field (H_{sf}) for **1**·$FeBr_4$ and **2**·$FeBr_4$.

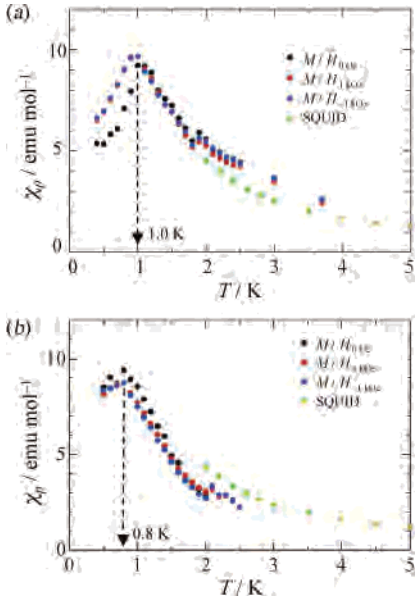

Figure 5. Temperature (T) dependences of magnetic susceptibilities (χ_p) measured at $H = 1$ kOe for (a) **1**·$FeCl_4$ and (b) **2**·$FeCl_4$ in the T region down to 0.5 K.

saturate at 5 μ_B with increasing H, which corresponds to the M value of the Fe(III) ($S = {}^5/_2$) d spins (Figure 4), indicating again that only the d spins contribute to the observed M values because the π spins on the donor molecules are placed in the singlet state. In the M curves of **1**·$FeBr_4$ and **2**·$FeBr_4$, an abrupt increase in M due to a spin-flop was observed near 2 kOe (the inset of Figure 4). On the other hand, such a spin-flop was not observed for **1**·$FeCl_4$ and **2**·$FeCl_4$ down to 1.9 K.

3.4. Antiferromagnetic or Canted Antiferromagnetic Orderings of the Short-Range Ferromagnetic d-Spin Chains in the Low-Temperature Region. To clear the magnetic behaviors of all of the salts below 1.9 K, the measurements of χ_p and M were carried out down to 0.4 K by use of a ^{3}He cryostat. Figure 5 shows the temperature dependences of χ_p for **1**·$FeCl_4$ (Figure 5a) and **2**·$FeCl_4$ (Figure 5b). The maxima in χ_p appeared at 1.0 and 0.8 K for **1**·$FeCl_4$ and **2**·$FeCl_4$, respectively, which can be regarded

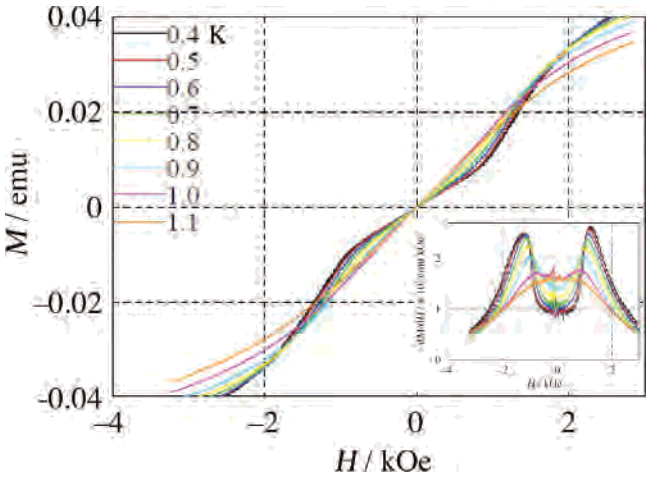

Figure 6. Field (H) dependences of magnetizations (M) in the H region of +3 to −4 kOe at different T's of 0.4−1.1 K for **1**·$FeCl_4$. The inset shows H dependences of dM/dH.

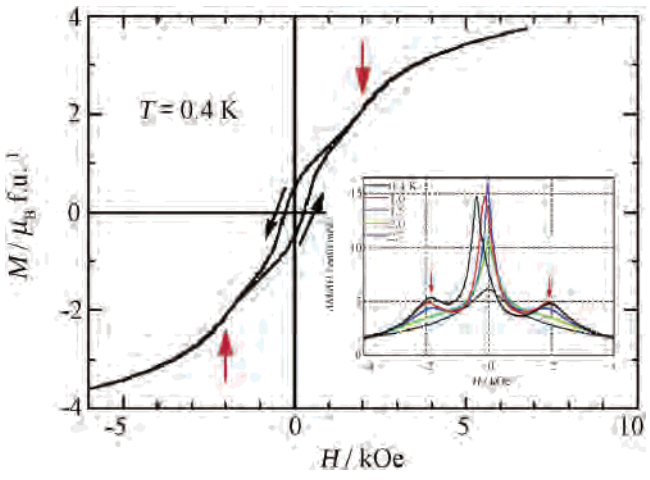

Figure 7. Field (H) dependence of magnetizations (M) in the $H = \pm 6$ kOe region at $T = 0.4$ K for **2**·$FeBr_4$. The inset shows H dependences of dM/dH in the $H = \pm 4$ kOe region at $T = 0.4$, 1.0, 1.5, 2.0, and 2.7 K. The arrows show spin-flops.

as their antiferromagnetic ordering temperatures. The $M-H$ curves in the temperature range down to 0.4 K were also measured for all of the salts. Figure 6 shows the $M-H$ and dM/d$H-H$ curves for **1**·$FeCl_4$. The $M-H$ curves were smooth S-shaped until 1.1 K, but at 1.0 K, the sharp increase in M due to the spin-flop suddenly began to occur near ±1.2 kOe and became remarkable with decreasing temperature (Figure 6). This threshold temperature of the spin-flop corresponds to the antiferromagnetic ordering temperature, which was determined to be 1.0 K by the χ_p-T experiment (Figure 5a). The change in the $M-H$ behaviors in the temperature range of 0.4−0.9 K can be much clearer by the dM/d$H-H$ plots. Similar $M-H$ and dM/d$H-H$ curves were also obtained for **2**·$FeCl_4$ except for a different threshold temperature (0.8 K) and H (±1.1 kOe) of the spin-flop. For **1**·$FeBr_4$, the antiferromagnetic ordering was already completed at 2.4 K, so that the accompanied spin-flop at $H = \pm 2.2$ kOe appeared in the $M-H$ curves at any temperature below 1.9 K.

As mentioned above, for **2**·$FeBr_4$, χ_p became constant near 2 K. To confirm the magnetic ordering and to determine the ordering temperature for **2**·$FeBr_4$, a resonant circuit method developed by us very recently was used,[17] which is quite useful in the case of ferromagnets with very low ordering temperature. In this measurement, a steplike change with a start near 2.0 K and a final near 1.5 K was obtained.[7] If the ordering temperature is defined as the midpoint of the steplike change, the value is determined to be 1.8 K. In the $M-H$ and dM/d$H-H$ curves below 1.5 K, a hysteresis was observed in the H range of ±1.5 kOe and a spin-flop at $H = \pm 2$ kOe, respectively (Figure 7). This weak ferromagnetic behavior originates from a canted antiferromagnetism, in which the spins are antiferromagnetically ordered by some canted angle to each other. The canted angle is roughly estimated to be ca. 6° from the remanent M value (ca. 0.5 μ_B) at $H = 0$ Oe. The hysteresis became larger with decreasing temperature from 1.5 K, but even at 0.4 K, the $M-H$ curve with the hysteresis appeared together with an S-shaped $M-H$ curve with no hysteresis at $H = \pm 2$ kOe. The coercive field at 0.4 K was determined to be ca. 400 Oe. The spin-flop appeared only below 1.9 K, and the applied H was almost the same as that (±2.2 kOe) observed for **1**·$FeBr_4$. Furthermore, the $M-H$ curve up to $H = 300$ kOe for **2**·$FeBr_4$ was measured, and the saturation in M occurred near $H = 100$ kOe and the M value was very close to 5 μ_B, which corresponds to only that of an Fe(III) ($S = {}^5/_2$) d-spin entity with no contribution of the π spins on the donor molecule.[7] Eventually, this canted antiferromagnetic ordering of **2**·$FeBr_4$ is of much interest and presents a striking contrast to antiferromagnetic orderings for the other three salts. The results of the θ values, magnetic orderings, magnetic ordering temperatures, and spin-flop fields for **1**·$FeCl_4$, **2**·$FeCl_4$, **1**·$FeBr_4$, and **2**·$FeBr_4$ are summarized in Table 2.

Table 2. Weiss Temperatures (θ), Magnetic Orderings, Magnetic Ordering Temperatures, and Spin-Flop Magnetic Fields (H_{sf}) for **1**·$FeCl_4$, **2**·$FeCl_4$, **1**·$FeBr_4$, and **2**·$FeBr_4$

salt	θ/K	magnetic ordering[a]	magnetic ordering temp/K	H_{sf}/kOe
1·$FeCl_4$	+1.8	AF	1.0	1.2
2·$FeCl_4$	+1.6	AF	0.8	1.1
1·$FeBr_4$	+3.7	AF	2.4	2.2
2·$FeBr_4$	+3.4	CAF	1.9	2.0

[a] AF and CAF denote antiferromagnetic and canted antiferromagnetic orderings, respectively.

3.5. Heat Capacity for 2·$FeBr_4$. The heat capacity (C) of **2**·$FeBr_4$ was measured at each applied H of 0, 1, 2, 3, and 4 kOe in the temperature range of 0.5−20 K (Figure 8). With decreasing temperature, the C value due to the lattice and/or electronic contributions sharply decreased. At $H = 0$ Oe, a gradual increase in C occurred near 3 K with decreasing temperature and reached a maximum near 2 K, and below the temperature, there was again a sharp decrease in C with decreasing temperature. This temperature dependence of C can be ascribed to an exothermic process due to the magnetic ordering of the Fe(III) d spins of the $FeBr_4^-$ ions. However,

(17) (a) Noguchi, S.; Matsumoto, A.; Matsumoto, T.; Sugimoto, T.; Ishida, T. *Physica B* **2004**, *346*−*347*, 397−401. (b) Noguchi, S.; Kosaka, T.; Wang, M.; Fujiwara, H.; Sugimoto, T.; Ishida, T. *AIP Conf. Proc. LT24* **2006**, *850*, 1063−1064.

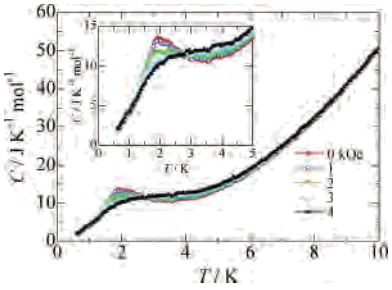

Figure 8. Temperature (T) dependences of heat capacities (C) in the T region of 0.5−10 K at H = 0, 1, 2, 3, and 4 kOe for **2**·$FeBr_4$. The inset shows an expansion in the T region lower than 5 K.

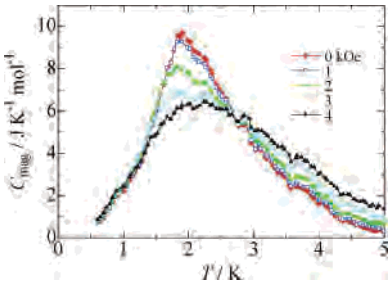

Figure 9. Temperature (T) dependences of magnetic heat capacities (C_{mag}) in the T region of 0.5−5 K at H = 0, 1, 2, 3, and 4 kOe for **2**·$FeBr_4$.

the peak of the $C-T$ behavior is not like the usual λ shape, suggesting a low dimensionality of the phase transition, but is so round that it seems to be an overlap of two peaks at very close temperatures around 2 K.

The contribution due to the lattice and/or electronic heat capacities was subtracted from the observed C value to give the magnetic heat capacity (C_{mag}). The temperature dependence of C_{mag} is also shown in Figure 9. As seen from Figures 8 and 9, two overlapped peaks with the temperature difference of <1 K are observed at H = 0 Oe. The $C_{mag}-T$ behavior at H = 1 kOe was very close to that at H = 0 Oe. However, at 2 kOe of the spin-flop H, the mountain-like shape became slightly more round and extended to a slightly higher temperature side, accompanied with a large decrease of the height, but the overlapped peaks still remained in the shape. At much higher H, the shape became much more round and extended to a much higher temperature side, and the two peaks completely collapsed. On the whole, the two peaks show very similar H dependences, suggesting that the corresponding magnetic orderings well resemble each other. This H dependence of the $C_{mag}-T$ behavior is quite in contrast with that observed by an $FeBr_4^-$ salt of ethylenedithiotetrathiafulvalenoquinone-1,3-dithiolemethide (EDT-TTFVO), (EDT-TTFVO)$_2$·$FeBr_4$, which exhibits a ferrimagnetic ordering at 1 K.[3d]

3.6. Estimation of Magnitudes of $\pi-$d and d−d Interactions ($J_{\pi d}$ and J_{dd}) for 1·$FeCl_4$, 2·$FeCl_4$, 1·$FeBr_4$, and 2·$FeBr_4$. The magnetic interactions between molecule **1** or **2** and the $FeCl_4^-$ or $FeBr_4^-$ ion ($\pi-$d interaction) and between the $FeCl_4^-$ or $FeBr_4^-$ ions (d−d interaction) were estimated using an extended Hückel MO method for the four salts.[18] First of all, the overlap integrals of the $\pi-$d ($S_{\pi d}$: ***1***, ***2***, ***3***, and ***4***) and d−d (S_{dd}: ***I***) interactions (Figure 2) were calculated using the crystal structure data. The $S_{\pi d}$ and S_{dd} values are shown in Table 3. The magnitudes of the $\pi-$d and d−d interactions ($J_{\pi d}$ and J_{dd}) can be expressed by equations of $J_{\pi d} = -(2t_{\pi d}^2)/\Delta_{\pi d}$ and $J_{dd} = -(2t_{dd}^2)/U_d$, respectively, where $t_{\pi d}$ and t_{dd} are transfer integrals between the HOMO of the donor molecules and the d MO of the $FeCl_4^-$ or $FeBr_4^-$ ion and between the d MO, respectively, $\Delta_{\pi d}$ is the energy difference between the HOMO of the donor molecules and the d MO, and U_d is the on-site Coulomb interaction on the d MO. $t_{\pi d}$ and t_{dd} are related to $S_{\pi d}$ and S_{dd} by $t_{\pi d} = ES_{\pi d}$ and $t_{dd} = ES_{dd}$, respectively, in which E, the HOMO energy level, is taken to be −10 eV. Usually, $J_{\pi d}$ and J_{dd} are obtained by the average of the five $\pi-$d interactions and of 5 × 5 = 25 combinations of the d−d overlaps, respectively, and they can be calculated using the following equations:

$$J_{\pi d} = \frac{1}{5}\sum_{i=1}^{5} J_{i,\pi d} = \frac{2}{5\Delta_{\pi d}}\sum_{i=1}^{5}(E,S_{i,\pi d})^2$$

$$J_{dd} = \frac{1}{25}\sum_{i=1}^{25} J_{i,dd} = \frac{2}{25U_d}\sum_{i=1}^{25}(E,S_{i,dd})^2$$

The $J_{\pi d}$ and J_{dd} values of the $\pi-$d and d−d interactions were calculated using $S_{\pi d}$ and S_{dd} as above, and the results are also shown in Table 3. The $\pi-$d interaction ***1*** has a very large $-J/k_B$ value (11.91−35.93 K) compared with the other ones for all of the salts, and comparatively large $-J/k_B$ values are also obtained for the $\pi-$d interaction ***2*** (1.82−7.61 K) and the d−d interaction ***I*** (0.45−2.07 K), in which the former is 4−6 times larger than the latter. The $\pi-$d interactions ***3*** and ***4*** have very small values. These calculated J values suggest that the neighboring Fe(III) d spins of the FeX_4^- ions interact with each other preferentially through the strong $\pi-$d interactions ***1*** and ***2*** rather than through the direct d−d interaction ***I***. Accordingly, in this spin system under the above circumstances, all of the d spins of the FeX_4^- ions have the same orientation, while all of the π spins of the donor molecules are aligned to the reverse orientation (Figure 10). Eventually, a ferromagnetic interaction is preferential for each d-spin chain along the a axis in such a high-temperature region that there is still weak interaction between the ferromagnetic d-spin chains. The neighboring d-spin chain is also located on the other side of the donor dimer layer, so that a pair structure of the ferromagnetic d-spin chains is formed. In addition, both J values of the $\pi-$d interactions ***1*** and ***2*** for the $FeBr_4^-$ salts are larger than those for the corresponding $FeCl_4^-$ salts, suggesting that the stronger ferromagnetic interaction is expected for the $FeBr_4^-$ salts than for the $FeCl_4^-$ salts. These predictions obtained by the MO calculations are well consistent with the experimental results of the positive θ values for all of the salts and higher θ values for the $FeBr_4^-$ salts than for the $FeCl_4^-$ salts.

In a lower temperature region, two ferromagnetic d-spin chains located on both sides of the donor dimer layer have reverse spin orientations to each other through the antiferro-

(18) Mori, T.; Katsuhara, M. *J. Phys. Soc. Jpn.* **2002**, *71*, 826−844.

Table 3. Overlap Integrals ($S \times 10^{-3}$) and Spin-Exchange Interactions ($-Jk_B^{-1}$/K) of $\pi-$d (***1***, ***2***, ***3***, and ***4***) and d−d (***I***) Interactions between Molecule **1** or **2** and the $FeCl_4^-$ or $FeBr_4^-$ Ion for **1**·$FeCl_4$, **2**·$FeCl_4$, **1**·$FeBr_4$, and **2**·$FeBr_4$

	1·$FeCl_4$		**2**·$FeCl_4$		**1**·$FeBr_4$		**2**·$FeBr_4$	
interaction	$S \times 10^{-3}$	$-Jk_B^{-1}$/K	$S \times 10^{-3}$	$-Jk_B^{-1}$/K	$S \times 10^{-3}$	$-Jk_B^{-1}$/K	$S \times 10^{-3}$	$-Jk_B^{-1}$/K
				$\pi-$d Interaction				
1	4.91	11.91	5.67	14.92	8.80	35.93	6.19	17.78
2	2.80	3.64	1.98	1.82	4.05	7.61	2.83	3.72
3	0.09	0.004	0.12	0.01	0.08	0.003	0.19	0.02
4	0.39	0.07	1.08	0.54	0.89	0.37	0.62	0.18
				d−d Interaction				
I	2.50	0.58	2.19	0.45	4.72	2.07	3.28	1.00

magnetic $\pi-$d interaction ***1*** and $\pi-\pi$ interaction ***c***, as shown in Figure 10. Accordingly, an antiferromagnetic ordering of the Fe(III) d spins of the FeX_4^- ions is expected to preferentially occur at low temperatures, and such a magnetic ordering was indeed realized for **1**·$FeCl_4$, **2**·$FeCl_4$, and **1**·$FeBr_4$ and also for **2**·$FeBr_4$, in which the antiferromagnetic ordering, however, occurs with some canted angle to leave a small magnetization. Their ordering temperatures were 1.0, 0.8, 2.4, and 1.9 K, respectively, which well correspond to the magnitudes of the interactions ***1*** and ***c*** (Tables 1 and 3). Nevertheless, it still remains unknown about the cause of the canted antiferromagnetic ordering for **2**·$FeBr_4$ at present, but supposedly the crystal structure of **2**·$FeBr_4$ may be subject to such a significant change at low temperature that two d-spin chains on both sides of the donor layer are somewhat inclined to each other.

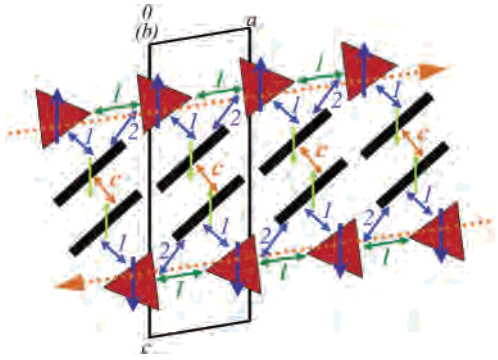

Figure 10. Schematic drawing of an antiferromagnetic interaction between neighboring ferromagnetic chains of the Fe(III) d spins of the $FeCl_4^-$ or $FeBr_4^-$ ions through the singlet π spins on molecule **1** or **2**.

4. Conclusion

In all of the salts composed of **1** or **2** and FeX_4^- ions, the π spins on the donor molecules are in the singlet state as the result of a strong dimer formation. On the other hand, the d spins of the FeX_4^- ions interact with each other by participation of one of the singlet π spins on the donor molecules to form short-range ferromagnetic d-spin chains, which are successively subject to antiferromagnetic interaction at lower temperatures. For the other salts, except for **2**·$FeBr_4$, the neighboring ferromagnetic d-spin chains make their spin directions completely antiparallel to each other, giving rise to antiferromagnetic orderings. However, for **2**·$FeBr_4$, such a complete antiparallel alignment is not achieved, so that a small remanent magnetization can arise. It is supposed that this canted antiferromagnetism originates from symmetry breaking between the neighboring ferromagnetic d-spin chains in the crystal at low temperatures. However, the reason why such a change in the crystal structure occurs only in **2**·$FeBr_4$ even though all of the salts have almost the same crystal structure to each other at room temperature is not known yet at present. Furthermore, the heat capacity measurement of **2**·$FeBr_4$ suggested the possibility of another magnetic ordering at a slightly higher temperature than 2 K. Very recently, a similar observation was obtained by the first muon spin rotation and heat capacity measurements of a molecular ferrimagnet, TTF·[$Cr(NCS)_4$(1,10-phenanthroline)], which showed two ordering transitions at 2 and 8.3 K.[19] This cause is also not understood yet. Anyway, the magnetic properties observed in the present 1:1 salts, in particular **2**·$FeBr_4$, presented a striking contrast to those of the previous 1:1 salts of TTF or its derivatives with $[M(NCS)_4(isoquinoline)_2]^-$ (M = Cr, Fe)[20] or [$Cr(NCS)_4$-(1,10-phenanthroline)]$^-$ ions,[21] in which both of the donor π spins and the counteranion d spins survive and contribute to the ferrimagnetism in these salts.

Acknowledgment. This work was financially supported in part by Grants-in-Aid for Scientific Research (Grants 16038222 and 17540336) from the Ministry of Education, Culture, Sports, Science and Technology of Japan.

Supporting Information Available: X-ray crystallographic file for the crystals of **1**·$FeCl_4$, **2**·$FeCl_4$, **1**·$FeBr_4$, and **2**·$FeBr_4$ in CIF format, projections of crystal structures of **2**·$FeCl_4$, **1**·$FeBr_4$, and **2**·$FeBr_4$ to the *bc* plane, temperature dependence of ESR signal intensities for **2**·$GaBr_4$, and *H* dependences of *M* and d*M*/d*H* in the *H* region of ±6 kOe at different *T*'s of 0.5−1.1 K for **2**·$FeCl_4$ and in the *H* region of +4 to −6 kOe at different *T*'s of 0.5−1.0 K for **1**·$FeBr_4$. This material is available free of charge via the Internet at http://pubs.acs.org.

IC0617700

(19) Day, P.; Carling, S. G.; Turner, S. S.; Bradley, J.; D. Hautot, D.; Visser, D. *ISIS Annual Report (Science Highlights)*; CCLRC Rutherford Appleton Laboratory: Didcot, Oxfordshire, U.K., 2003; p 8.

(20) (a) Turner, S. S.; Michaut, C.; Durot, S.; Day, P.; Gelbrich, T.; Hursthouse, M. B. *J. Chem. Soc., Dalton Trans.* **2000**, 905−909. (b) Setifi, F.; Golhen, S.; Ouahab, L.; Turner, S. S.; Day, P. *Cryst. Eng. Commun.* **2002**, *4*, 1−6. (c) Setifi, F.; Golhen, S.; Ouahab, L.; Miyazaki, A.; Okabe, K.; Enoki, T.; Toita, T.; Yamada, J. *Inorg. Chem.* **2002**, *41*, 3786−3790. (d) Mas-Torrent, M.; Turner, S. S.; Wurst, K.; Vidal-Gancedo, J.; Ribas, X.; Veciana, J.; Day, P.; Rovira, C. *Inorg. Chem.* **2003**, *42*, 7544−7549. (e) Zhang, B.; Wang, Z.; Fujiwara, H.; Kobayashi, H.; Kurmoo, M.; Inoue, K.; Mori, T.; Gao, S.; Zhang, Y.; Zhu, D. *Adv. Mater.* **2005**, *17*, 1988−1991.

(21) (a) Turner, S. S.; Le Pevelen, D.; Day, P.; Prout, K. *J. Chem. Soc., Dalton Trans.* **2000**, 2739−2744. (b) Le Pevelen, D.; Turner, S. S.; Day, P.; Prout, C. K. *Synth. Met.* **2001**, *120*, 1842−1843. (c) Turner, S. S.; Carling, S.; Day, P.; Gómez Garciá, C. J.; Coronado, E. *J. Phys. IV* **2004**, *114*, 585−587.